SHARC-II 350μm Observations of Thermal Emission from Warm Dust in z$\geq$5 Quasars

Ran Wang[1,2], Jeff Wagg[2], Chris L. Carilli[2], Dominic J. Benford[3], C. Darren Dowell[4], Frank Bertoldi[5], Fabian Walter[6], Karl M. Menten[7], Alain Omont[8], Pierre Cox[9], Michael A. Strauss[10], Xiaohui Fan[11], Linhua Jiang[11]

ABSTRACT

We present observations of four z $\geq$ 5 SDSS quasars at 350 μm with the SHARC-II bolometer camera on the Caltech Submillimeter Observatory. These are among the deepest observations that have been made by SHARC-II at 350 μm, and three quasars are detected at $\geq 3\sigma$ significance, greatly increasing the sample of 350 μm (corresponds to rest frame wavelengths of $< 60\,\mu$m at z $\geq$ 5), detected high-redshift quasars. The derived rest frame far-infrared (FIR) emission in the three detected sources is about five to ten times stronger than that expected from the average SED of the local quasars given the same 1450 Å luminosity. Combining the previous submillimeter and millimeter observations at longer wavelengths, the temperatures of the FIR-emitting warm dust from the three quasar detections are estimated to be in the range of 39 to 52 K. Additionally, the FIR-to-radio SEDs of the three 350 μm detections are consistent with the emission from typical star forming galaxies. The FIR luminosities are $\sim 10^{13}\,L_\odot$ and the dust masses

[1]Department of Astronomy, Peking University, Beijing 100871, China

[2]National Radio Astronomy Observatory, PO Box 0, Socorro, NM, USA 87801

[3]NASA / Goddard Space Flight Center, Code 665 - Observational Cosmology Lab, Greenbelt, MD, USA 20771

[4]Jet Propulsion Laboratory, Mail Code 169-506, Pasadena, CA, USA 91109

[5]Argelander-Institut für Astronomie, University of Bonn, Auf dem Hügel 71, 53121 Bonn, Germany

[6]Max-Planck-Institute for Astronomy, Königsstuhl 17, 69117 Heidelberg, Germany

[7]Max-Plank-Institute for Radioastronomie, Auf dem Hügel 71, 53121 Bonn, Germany

[8]Institut d'Astrophysique de Paris, CNRS and Universite Pierre et Marie Curie, Paris, France

[9]Institute de Radioastronomie Millimetrique, St. Martin d'Heres, F-38406, France

[10]Department of Astrophysical Sciences, Princeton University, Princeton, NJ, USA, 08544

[11]Steward Observatory, The University of Arizona, Tucson, AZ 85721

are $\geq 10^8\,M_\odot$. These results confirm that huge amounts of warm dust can exist in the host galaxies of optically bright quasars as early as z∼6. The universe is so young at these epochs ($\sim 1\,$Gyr) that a rapid dust formation mechanism is required. We estimate the size of the FIR dust emission region to be about a few kpc, and further provide a comparison of the SEDs among different kinds of dust emitting sources to investigate the dominant dust heating mechanism.

Subject headings: galaxies: high-redshift — galaxies: starburst — infrared: galaxies — submillimeter — quasars: individual (SDSS J033829.31+002156.3, SDSS J075618.14+410408.6, SDSS J092721.82+200123.7, SDSS J104845.05+463718.3)

1. Introduction

Quasars in the distant universe may be studied as important probes of supermassive black hole (SMBH) and host galaxy formation at early epochs. Universal relationships between the supermassive black holes (SMBHs) and their stellar bulges were found in both active and normal galaxies locally, indicating that the early evolution of the SMBH-bulge systems is tightly correlated (eg. Marconi & Hunt 2002; Tremaine et al. 2002). How these relationships behaved at an early galaxy evolution stage is a critical question for the studies of the high-z universe. In particular, if the SMBH forms prior to the stellar bulge, we may expect to see massive star formation co-eval with rapid black hole accretion in the quasar systems at the highest redshifts.

Observations at submillimeter and millimeter [(sub)mm] wavelengths were preformed to study the thermal emission from warm dust in the quasar host galaxies at high redshifts. These studies yield important information on the mass and temperature of the FIR-emitting dust, and thus provide key constraints on the related galaxy evolution activities. Samples of optically bright quasars from z∼2 to 6 have been observed at (sub)mm wavelengths (Omont et al. 1996; Omont et al. 2001; 2003, Carilli et al. 2001; Beelen et al. 2003; Bertoldi et al. 2003a; Priddey et al. 2003a, Robson et al. 2004; Wang et al. 2007), using the Max-Planck Millimeter Bolometer (MAMBO) on the IRAM-30m Telescope and the Submillimeter Common-User Bolometer Array (SCUBA) on the James Clerk Maxwell Telescope. The detection rate is about 30% at mJy sensitivity for all these samples, indicating the existence of a population of FIR luminous objects within the high-z optically selected quasar sample.

Important results were obtained from deep 350 μm observations of these strong (sub)mm quasars (Benford et al. 1999; Beelen et al. 2006) made by the SHARC-II bolometer camera (Dowell et al. 2003) on the Caltech Submillimeter Observatory (CSO). The 350 μm obser-

vations confirm the existence, and constrain the properties of the warm dust with a typical temperature of $\sim 50\,\mathrm{K}$ in the host galaxies of these quasars (Benford et al. 1999; Beelen et al. 2006). Fits of the FIR (SEDs) imply FIR luminosities of about $\sim 10^{13}\,\mathrm{L}_\odot$ and FIR-to-radio luminosity ratios following the trend defined by star forming galaxies (Beelen et al. 2006). These properties are all comparable to the FIR emission found in the submillimeter detected galaxies (SMGs) at z$\sim$1 to $\gtrsim$3, i.e. thermal emission from >10 K to 70 K warm dust heated by star formation at a rate of a few $10^3\,\mathrm{M}_\odot\,\mathrm{yr}^{-1}$ (eg. Chapman et al. 2005; Kovács et al. 2006b). The SHARC-II detected quasars also tend to have highly excited molecular CO emission from the host galaxies (i.e. peak at $\mathrm{J} = 6 - 5$ or higher, Carilli et al. 2002, 2007; Solomon & Vanden Bout 2005), exhibiting FIR-to-CO emission ratios similar to that of the star forming galaxies at low and high redshifts (Solomon & Vanden Bout 2005; Riechers et al. 2006; Carilli et al. 2007).

One instrumental finding among these observations is the SHARC-II detection of SDSS J114816.64+525150.3 at z=6.42 (hereafter J1148+5251, Beelen et al. 2006). This is the first $350\,\mu$m dust continuum detection beyond z = 5. The $4.5 \times 10^8\,\mathrm{M}_\odot$ of $\sim$ 55K warm dust discovered in this source implies a similar evolution stage as was found in other (sub)mm detected quasars at lower redshifts, but exist at an epoch when the age of the universe is only $\sim$870 Myr. Probing the warm dust emission at such an epoch is critical as it constrains the time scale of dust formation in addition to the questions of dust heating and black hole-bulge evolution. The detection of J1148+5251 indicates a rapid dust formation in these earliest galaxies (forming $\geq 10^8\,\mathrm{M}_\odot$ of dust within $\leq$1 Gyr), which requires confirmation with more examples at similar redshifts.

In this paper, we report our new $350\,\mu$m SHARC-II observations of four z$\geq$5 SDSS quasars. These quasars are among the strongest MAMBO 1.2 mm detections at z$\geq$5 (Carilli et al. 2001; Petric et al. 2003; Priddey et al. 2003b; Bertoldi et al. 2003a; Wang et al. 2007). The observations presented in this work are among the most sensitive ones that have been made by SHARC-II at $350\,\mu$m, and are of critical importance as they deliver a data point on the short wavelength side or near the peak of the redshifted FIR emission spectrum. Combining with measurements on the long wavelength side allows determination of the dust temperature and, thus, the mass and the FIR luminosity. We describe the SHARC-II observations in Section 2, list the results in Section 3, and present discussions in Section 4. We adopt a Λ-model cosmology with $\mathrm{H}_0 = 71\mathrm{km\ s}^{-1}\ \mathrm{Mpc}^{-1}$, $\Omega_\mathrm{m} = 0.27$ and $\Omega_\Lambda = 0.73$ (Spergel et al. 2007), throughout this paper.

2. Observations

The observations were carried out with SHARC-II on the 10.4 m telescope of the CSO during 2007 January 13-18 UT. The SHARC-II camera is a 12×32 pixel array with a beam size (FWHM) of $8.5''$ at $350\,\mu$m. The field of view is $2.6' \times 1.0'$. We observed the four target sources when the opacity at 225GHz ($\tau_{225\mathrm{GHz}}$) was ≤ 0.06, i.e. during the best weather conditions on Mauna Kea. The CSO Dish Surface Optimization System (DSOS, Leong 2005) was used to correct the surface imperfections and gravitational deformations. Scans were performed using a Lissajous pattern with amplitudes of $\pm 45''$ and $\pm 12''$ in azimuth and elevation respectively, resulting in a uniform coverage of $\sim 65'' \times 34''$. We performed hourly pointing, focus, and flux calibration with strong sources. We used Uranus as a primary calibrator, and a number of sources, IRC10216, CRL618, CIT6, OH231.8+4.2, GL490, and Arp220 were used as secondary calibrators. The uncertainties of the final calibration were expected to be within 20%, based on repeated observations of the calibrators and the flux uncertainties of the secondary calibrators. The 1σ pointing uncertainties, estimated from repeated pointing on calibrators, is about $2.3''$.

During standard observing, the position of the secondary mirror is updated frequently to compensate for sag as the telescope elevation changes. Unfortunately, a telescope configuration problem on the last three nights resulted in only infrequent updates. The effects of this problem are a drift in the focus and a small drift in pointing. We carefully studied the effects of the mirror position errors on the data using the position encoders and images of the calibrators. About half of the data was dropped due to bad focus. For the remaining data, we made small ($< 3''$) adjustments to the pointing with an uncertainty of $< 1''$.

We completed data reduction using the SHARC-II data reduction package CRUSH version 1.52 (Kovàcs 2006a). The total integration time for each source is about 6 to 8 hours after excluding the bad scans, and the rms noise level for the final maps is about 5 to 6 mJy beam^{-1}. The final maps were smoothed to a FWHM of $12.4''$, for optimal signal-to-noise in the case of point-source detection, and the peak surface brightness is adopted as the total flux density of the source.

3. Results

Three out of the four z$\geq$5 quasars observed are detected at the $\gtrsim 3\sigma$ level with SHARC-II. We list basic information and previous (sub)mm and radio continuum results of the four targets in Table 1, and the results of the SHARC-II observations are presented in the first four columns of Table 2, including the source name, 350μm peak surface brightness, peak offset

from the optical quasar, and the integration time. The final SHARC-II maps of all the four targets are presented in Figure 1. The 1σ position uncertainty on the map is $\sigma_{\rm pos} \sim \frac{\rm FWHM}{\rm SNR} \sim 4''$ for 3σ detections (considering the smoothed beam size of FWHM = $12.4''$). Thus the $350\,\mu$m peak positions of the three detections are consistent with the optical quasars given this position uncertainty (See Column 3 in Table 2). The details for the individual sources are presented in the following.

J033829.31+002156.3 (hereafter J0338+0021) is a z=5.03 quasar discovered by Fan et al. (1999). It is one of the strongest MAMBO detections among a sample of z$\geq$ 4 SDSS quasars from Carilli et al. (2001) with $\rm S_{\nu,1.2mm} = 3.7 \pm 0.3\,mJy$. The dust continuum is also detected by SCUBA at $850\,\mu$m (Priddey et al. 2003b). Moreover, Maiolino et al. (2007) detected CO(5-4) line emission in this source, with a molecular gas mass of $2.4 \times 10^{10}\,\rm M_\odot$.

This source is detected by our SHARC-II observation at the $\sim 4\sigma$ level, with a peak surface brightness of $\rm S_{\nu,350\mu m} = 17.7 \pm 4.4\,mJy\,beam^{-1}$ $3.8''$ away from the optical position.

J075618.14+410408.6 (hereafter J0756+4104) was discovered by Anderson et al. (2001) with a redshift of z=5.09. It is a strong MAMBO source with $\rm S_{\nu,1.2mm} = 5.5 \pm 0.5\,mJy$ (Petric et al. 2003), and also is detected at $450\,\mu$m and $850\,\mu$m by SCUBA (Priddey et al. 2003b; Priddey et al. 2007) and at 1.4GHz by the VLA (Petric et al. 2003).

We detect a 3.3σ peak ($\rm S_{\nu,350\mu m} = 17.1 \pm 5.2\,mJy\,beam^{-1}$) on the SHARC-II map, $4.3''$ away from the position of the optical quasar.

J092721.82+200123.7 (hereafter J0927+2001) is a SDSS quasar at z=5.77 (Fan et al. 2006b; Carilli et al. 2007). This source has a MAMBO flux density of $\rm S_{\nu,1.2mm} = 5.0 \pm 0.8\,mJy$, making it one of the most luminous quasars at z$\sim$6 at FIR wavelengths (Wang et al. 2007). The VLA radio continuum observation of this source yields a 3σ detection of $\rm S_{1.4GHz} = 45 \pm 14\,\mu Jy$ at 1.4GHz. CO(5-4) and CO(6-5) line emission has also been detected in this source very recently (Carilli et al. 2007). The CO luminosity indicates molecular gas with a mass of $1.6 \times 10^{10}\,\rm M_\odot$ in the host galaxy. The CO observations are accompanied with a $\sim 3\sigma$ continuum measurement at 3.5 mm of $\rm S_{\nu,3.5mm} = 0.12 \pm 0.03\,mJy$.

With SHARC-II we measure a brightness for this source of $\rm S_{\nu,350\mu m} = 17.7 \pm 5.7\,mJy\,beam^{-1}$ with a position offset of $3.9''$ from the optical quasar. A second $\sim 3\sigma$ peak is seen in the map of this source with $\rm S_{\nu,350\mu m} = 17.5 \pm 5.6\,mJy\,beam^{-1}$, to the southeast of the optical quasar position. The separation between the two peaks is about $14.9''$. However, there is no hint of extension towards the secondary peak direction in the CO emission maps of J0927+2001 at 3 mm of Carilli et al. (2007). Further high resolution mapping at (sub)mm wavelengths is required to understand the nature of this secondary peak. The analysis below only considers the first peak close to the optical quasar position.

J104845.05+463718.3 (hereafter J1048+4637) is a broad absorption line quasar at z=6.20 from Fan et al. (2003). The MAMBO flux density for this source is $S_{\nu,1.2mm} = 3.0 \pm 0.4$ mJy (Bertoldi et al. 2003). However, it has not been detected by SCUBA (Robson et al. 2004), or by the VLA (Wang et al. 2007).

Our SHARC-II observation did not detect this source. The pixel flux density value at the optical quasar position is 5.3 mJy beam^{-1}, with a 1σ rms of 5.8 mJy beam^{-1} on the final map. Thus we adopt 17.4 mJy beam^{-1} (3σ rms) as an upper limit to the 350 μm flux density.

The optical-to-radio SEDs of the four quasars are plotted in Figure 2, displaying the photometric data listed in Table 1 and 2. Template SEDs of local quasars from Elvis et al. (1994) and Richards et al. (2006) are plotted for comparison, normalized to 1450Å. For J1048+4637, the measurements at submillimeter, millimeter and radio wavelengths are all consistent with the templates, i.e. the average SED emission of the typical type-I quasar in the local universe. However, strong FIR emission is seen in the other three sources, which exceed the templates by nearly an order of magnitude. This is similar to the FIR excess from warm dust shown in the SED of J1148+5251 by Beelen et al. (2006).

We fit the FIR bumps of the three sources with an optically thin graybody, namely

$$S_\nu = S_0 \cdot \left(\frac{\nu}{1\mathrm{GHz}}\right)^{3+\beta} \frac{1}{\exp(h\nu/kT_d) - 1}, \quad (1)$$

where β is the emissivity index, T_d is the dust temperature in K, S_0 is the amplitude factor, and S_ν is the rest frame flux density in mJy. Since there are only two or three data points available for each source, we fix the β value to 1.6 (Beelen et al. 2006), and then fit S_0 and T_d for the three sources. A Levenberg-Marquardt least-squares fit is performed with the IDL package MPFIT. The best-fitting dust temperatures range from 39 to 52 K with 1σ fitting errors of 3 to 4 K. In Figure 2, we also extended the fitted FIR SED to radio for the three detections, using a radio spectral index of -0.75 and an average FIR-to-radio emission ratio of $q \equiv \log(L_{FIR}/3.75 \times 10^{12}\,\mathrm{W}) - \log(L_{\nu,1.4GHz}/\mathrm{W\,Hz^{-1}}) = 2.34$ found in typical star forming galaxies (Yun et al. 2001). The observed radio emission/upper limit of the three objects are all consistent with the model SED, i.e. within the range of FIR-to-radio emission ratios five times above or below the average value of star forming galaxies, but the detected flux densities in J0756+4104 and J0927+2001 are 0.2 to 0.4 index higher than the value derived with q=2.34.

The FIR luminosity is calculated from the fitted SED, integrating rest frame 42.5 μm to 122.5 μm, namely

$$L_{FIR} = 2.49 \times 10^{-11} \cdot 4\pi D_L^2 \int S_\nu d\nu \quad (2)$$

where D_L is the luminosity distance in Mpc and L_{FIR} is in $L_\odot$. We calculate the dust masses following

$$M_{dust} = \frac{L_{FIR}}{4\pi \int \kappa_\nu B_\nu d\nu} = 8.33 \times 10^{14} \cdot \frac{S_0 D_L^2}{\kappa_0} \, M_\odot \tag{3}$$

where B_ν is the planck function and $\kappa_\nu = \kappa_0(\nu/\nu_0)^\beta$ is the dust absorption coefficient. We adopt $\kappa_0 = 18.75\,cm^2g^{-1}$ at $125\,\mu m$ (Hildebrand 1983). The derived parameters for the three SHARC-II detected sources are listed in the last four columns in Table 2.

4. Discussion

We have detected three high redshift quasars with SHARC-II at $350\,\mu m$. These are among the most sensitive observations made by SHARC-II, and increase the number of $350\,\mu m$ detected optical quasars at z≥5 to four. These quasars are all strong detections in previous MAMBO and SCUBA observations at longer wavelengths (Carilli et al. 2001; Petric et al. 2003; Robson et al. 2004; Wang et al. 2007), and the measurements given by SHARC-II are close to the FIR emission peak from warm dust. By sampling over the dust peak, we provide reliable measurements of temperature, mass, and FIR luminosity of the FIR-emitting warm dust. As with J1148+5251, (Bertoldi et al. 2003; Beelen et al. 2006), the three newly detected sources show that excess emission from huge amounts of warm dust can exist in some optically bright quasars at extreme redshifts.

The derived dust masses are all $\geq 10^8\,M_\odot$. This result confirms the high heavy element abundance and rapid dust formation in massive quasar hosts at z≥5 (Priddey et al. 2003b; Bertoldi et al. 2003a) when the age of the universe was $\lesssim 1.2\,Gyr$. At this epoch, the standard mechanism of ISM dust formation, i.e. stellar winds from evolved low mass stars, is inefficient as it requires very long time scales ($> 1\,Gyr$). A process associated with the evolution of massive stars, (with a much shorter time scale), is likely required (eg. Morgan & Edmunds 2003; Schneider et al. 2004; Maiolino et al. 2004).

All of the SHARC-II detected z≥5 quasars exhibit FIR luminosities of $\sim 10^{13}\,L_\odot$. Under the optically thin assumption (i.e. the optical depth $\tau_\nu \ll 1$ at FIR wavelengths), the size of the dust emission region can be roughly estimated as

$$R_{dust} \sim [\frac{L_{FIR}}{(4\pi)(\pi \int \tau_\nu B_v(T_d \sim 50K)\, d\nu)}]^{0.5} \tag{4}$$

where the emissivity index $\beta = 1.6$, $\tau_\nu = (\nu/\nu_c)^\beta$, and ν_c is the critical frequency with $\tau_{\nu_c} = 1$. To satisfy the optically thin assumption, we adopt $\nu_c = 30\,THz$ (i.e. $\lambda_c = 10\,\mu m$).

The derived R_{dust} is ~ 5 kpc, which suggests the FIR-emitting warm dust emission region is on kpc scales in the quasar host. This is consistent with the scales of CO emission and [C II] 158 μm emission found in J1148+5251 (Walter, et al. 2004, 2007, in prep.).

The dust temperatures derived from these z≥5 quasars are in the range from 39 to 55 K, which is comparable to the values found in the bright (sub)mm quasars at lower redshifts (Benford et al. 1999; Beelen et al. 2006). They are also within the range of about 11 to 72 K found in samples of submillimeter selected galaxies at z∼1 to 3.5, but a little higher than the mean value of ∼35 K (Chapman et al. 2005; Kovács et al. 2006b). We combine the infrared to radio data of all four SHARC-II detected z≥5 quasars and plot them in Figure 3. The combined SED is compared to that of another two sources, the z=3.9 quasar APM 08279+5255 (Irwin et al. 1998; Lewis et al. 1998, 2002; Downes et al. 1999; Egami et al. 2000; Beelen et al. 2006; Wagg et al. 2005; Weiβ et al. 2007) and the local starburst galaxy M82 (Telesco & Harper 1980; Klein et al. 1988; Hughes et al. 1990; Smith et al. 1990; Krügel et al. 1990). The FIR emission from APM 08279+5255 is suggested to be dominated by a ∼200 K dust component on scales of a few hundred pc, i.e. a typical AGN heated hot dust torus (Weiβ et al. 2007), while the FIR emission in the starburst galaxy M82 is clearly from starburst heated warm dust with a temperature of ∼45 K (Klein et al. 1998). The combined FIR-to-radio emission of the four quasars can be probed by the SED of M82 very well, but is quite different from the dusty AGN emission from APM 08279+5255, which peaks at a shorter wavelength ($\sim 20\,\mu$m) and shows a much steeper infrared slope. Among the four z≥5 SHARC-II detections, only J1148+5251 have Spitzer measurements at near-IR wavelengths (Charmandaris et al. 2004; Jiang et al. 2006), and the flux densities are all much lower compared to the near-IR emission of APM 08279+5255.

The estimate of R_{dust} and the comparison of the IR SEDs may suggest a starburst origin of the strong FIR emission in these z≥5 quasars detected by SHARC-II and other (sub)mm detectors. If this is the case, the star formation rates derived from the FIR luminosities are all $\gtrsim 10^3\,M_\odot yr^{-1}$ (as listed in Col. (8), Table 2)[1], indicating an active bulge building in these quasar hosts. We expect future observations with Spitzer and the Herschel Space Observatory to better constrain the dust emission SEDs of these objects, and high resolution imaging ($\sim 1''$) with the Atacama Large Millimeter Array (ALMA) to constrain the size of the dust emission region These future observations will give a better understanding of star formation and warm dust heating in these high-z bright (sub)mm quasars.

[1]We estimate the star formation rate with the empirical relationship from Kennicutt (1998) assuming a standard initial mass function, i.e. SFR $\sim 4.5 L_{IR}\,M_\odot yr^{-1}$, where L_{IR} is the infrared luminosity (8-1000 μm) in unit of $10^{44}\,erg\,s^{-1}$, and is $\sim 1.5 L_{FIR}$ for warm dust emission.

We thank Jonathan Bird at the CSO for preparing the opacity data. We thank Colin Borys for helpful advice on SHARC-II data reduction. The CSO is supported by the NSF under AST-0540882. We acknowledge support from the Max-Planck Society and the Alexander von Humboldt Foundation through the Max-Planck-Forschungspreis 2005. The National Radio Astronomy Observatory is a facility of the National Science Foundation operated under cooperative agreement by Associated Universities, Inc.

Facilities: CSO (SHARC-II), IRAM (MAMBO), VLA, SDSS.

REFERENCES

Anderson, S. F. et al. 2001, AJ, 122, 503

Beelen, A., Cox, P., Benford, D. J., Dowell, C. D., Kovács, A., Bertoldi, F., Omont, A., & Carilli, C. L. 2006, ApJ, 642, 694 ApJ, 450, 559

Bertoldi, F., Carilli, C. L., Cox, P., Fan, X., Strauss, M. A., Beelen, A., Omont, A., & Zylka, R. 2003a, A& A, 406, L55

Bertoldi, F. et al. 2003b, A& A, 409, L47

Carilli, C. L. et al. 2001, ApJ, 555, 625

Carilli, C. L. et al. 2004, AJ, 128, 997

Carilli, C. L. et al. 2007, ApJL, in press, (astro-ph/0707.2339)

Chapman, S. C., Blain, A. W., Smail, I., & Ivison, R. J. 2005, ApJ, 622, 772

Charmandaris, V. et al. 2004, ApJS, 154, 142

Dowell, C. D. et al. 2003, Proc. SPIE, 4855, 73

Downes, D., Neri, R., Wiklind, T., Wilner, D. J., & Shaver, P. A. 1999, ApJ, 513, L1

Egami, E., Neugebauer, G., Soifer, B. T. & Matthews, K. 2000, ApJ, 535, 561

Elvis, M. et al. 1994, ApJS, 95, 1

Fan, X. et al. 1999, AJ, 118, 1

Fan, X. et al. 2003, AJ, 125, 1649

Fan, X., Carilli, C. L., & Keating, B. 2006a, ARA&A, 44, 415

Fan, X. et al. 2006b, AJ, 131, 1203

Fritz, J., Franceschini, A., & Hatziminaoglou, E. 2005, MNRAS, 366, 767

Helou, G., Soifer, B. T., & Rowan-Robinson, M. 1985, ApJ, 298, L7

Hughes, D. H., Gear, W. K., & Robson, E. I. 1990, MNRAS, 244, 759

Irwin, M. J., Ibeta, R. A., Lewis, G. F., & Totten, E. J. 1998, ApJ, 505, 529

Jiang, L. et al. 2006, AJ, 132, 2127

Kennicutt, R. C. 1998, ARA&A, 36, 189

Klein, U., Wielebinski, R., & Morsi, H. W. 1988 A&A 190,41

Krügel, E., Chini, R., Klein, U. et al. 1990, A&A, 240, 232

Kovács, A. 2006a, PhD thesis, Caltech

Kovács, A., Chapman, S. C., Dowell, C. D., Blain, A. W., Ivison, R. J., Smail, I., & Phillips, T. G., 2006b, ApJ, 650, 592

Leong M. M. 2005, URSI Conf. Sec., J3-J10, 426

Lewis, G. F., Chapman, S. C., Ibata, R. A., Irwin, M. J., & Totten, E. J., 1998, ApJ, 505, L1

Lewis, G. F., Carilli, C., Papadopoulos, P., Ivison, R. J. 2002, MNRAS, 330, L15

Maiolino, R., Schneider, R., Oliva, E., Bianchi, S., Ferrara, A., Mannucci, F., Pedani, M., & Roca, S. M. 2004, Nature,431,533

Maiolino, R. et al. 2007, A&A, in press

Morgan, H. L., & Edmunds, M. G., 2003, MNRAS, 343, 427

Omont, A., Cox, P., Bertoldi, F., Cox, P., Carilli, C. L., Priddey, R. S., McMahon, R. C., & Isaak, K. G. 2001, A&A, 374, 371

Omont, A., Beelen, A., Bertoldi, F., McMahon, R. G., Carilli, C. L., & Isaak, K. G. 2003, A&A, 398, 657

Petric, A. O., Carilli, C. L., Bertoldi, F., Fan, X., Cox, P., Strauss, M. A., Omont, A., & Schneider, D. P. 2003, AJ, 126, 15

Priddey, R. S., Isaak, K. G., McMahon, R. G., & Omont, A. 2003a, MNRAS, 339, 1183

Priddey, R. S., Isaak, K. G., McMahon, R. G., Roboson, E. I., & Pearson, C. P. 2003b, MNRAS, 344, L74

Priddey, R. S., Ivison, R. J., & Isaak, K. G. 2007, MNRAS, submitted, (astro-ph/0709.0610)

Richards, G. T. et al. 2006, ApJS, 166, 470

Riechers, D. A. et al. 2006, ApJ, 650, 604

Robson, I., Priddey, R. S., Isaak, K. G., & McMahon, R. G. 2004, MNRAS, 351, L29

Sanders, D. B., Phinney, E. S., Neugebauer, G., Soifer, B. T., & Mattherws, K. 1989, ApJ, 347, 29

Schneider, R., Ferrara, A., & Salvaterra, R. 2004, MNRAS, 351, 1379

Smith, P. A., Brand, P. W. J. L., Puxley, P. J., Mountain, C. M., & Nakai, N. 1990, MNRAS, 243, 97

Solomon, P. M., & Vanden Bout, P. A. 2005, ARA&A, 43, 677

Spergel, D. N. et al. 2007, ApJS, 170, 377

Telesco, C. M., & Harper, D. A. 1980, ApJ, 235, 392

Wagg, J., Wilner, D. J., Neri, R., Downew, D., & Wiklind, T. 2005, ApJ, 634, L13

Walter, F., Carilli, C. L., Bertoldi, F., Menten, K., Cox, P.,Lo, K. Y., Fan, X., & Strauss, M. A. 2004, ApJ, 615, L17

Walter, F. et al. 2007, in prep.

Wang, R. et al. 2007, AJ, 134, 617

Weiβ, A., Downes, D., Neri, R., Walter, F., Henkel, C., Wilner, D. J., Wagg, J., & Wiklind, T. 2007, A&A, 467, 955

Yun, M. S., Reddy, N. A., & Condon, J. J. 2001, ApJ, 554, 803

Table 1: Summary of the previous observations

SDSS name	z	$m_{1450\mathring{A}}$	$S_{\nu,450\mu m}$ mJy	$S_{\nu,850\mu m}$ mJy	$S_{\nu,1.2mm}$ mJy	$S_{\nu,3.5mm}$ mJy	$S_{1.4GHz}$ μJy
(1)	(2)	(3)	(4)	(5)	(6)	(7)	(8)
J033829.31+002156.3	5.03	20.01[a]	5±16[b]	11.9±2.0[b]	3.7±0.3[c]	—	37±25[c]
J075618.14+410408.6	5.09	20.15[d]	16±5[l]	13.4±1.0[l]	5.5±0.5[e]	—	65±17[e]
J092721.82+200123.7	5.77	19.87[f]	—	—	5.0±0.8[g]	0.12±0.03[k]	45±14[g]
J104845.05+463718.3	6.20	19.25[h]	7.6±11.7[i]	2.3±2.2[i]	3.0±0.4[j]	—	6±11[g]

[a]Fan et al. (1999). [b]Priddey et al. (2003b). [c]Carilli et al. (2001). [d]Anderson et al. (2001). [e]Petric et al. (2004). [f]Fan et al. (2006). [g]Wang et al. (2007). [h]Fan et al. (2003). [i]Robson et al. (2004). [j]Bertodi et al. (2003a). [k]Carilli et al. (2007). [l]Priddey et al. (2007)

Table 2: Results and derived parameters

SDSS name	$S^{a}_{\nu,350\mu m}$ mJy beam^{-1}	Offsets $''$	Int. time hours	L_{FIR} 10^{13} L$_\odot$	M_{dust} 10^{8} M$_\odot$	T_{dust} K	SFR 10^{3} M$_\odot$yr^{-1}
(1)	(2)	(3)	(4)	(5)	(6)	(7)	(8)
J033829.31+002156.3	17.7±4.4	3.8	7.2	0.92±0.17	6.1	45.6±3.2	2.2
J075618.14+410408.6	17.1±5.2	4.3	6.3	0.84±0.17	12.1	39.2±2.6	1.9
J092721.82+200123.7	17.7±5.7	3.9	7.3	1.21±0.28	4.6	51.1±4.2	3.2
J104845.05+463718.3	5.3 ± 5.8	—	8.0	—	—	—	—

[a] Note that the absolute calibration uncertainty of 20% is not included in the rms.

We adopt an emissivity index of $\beta = 1.6$ here for all the calculations (Beelen et al. 2006).

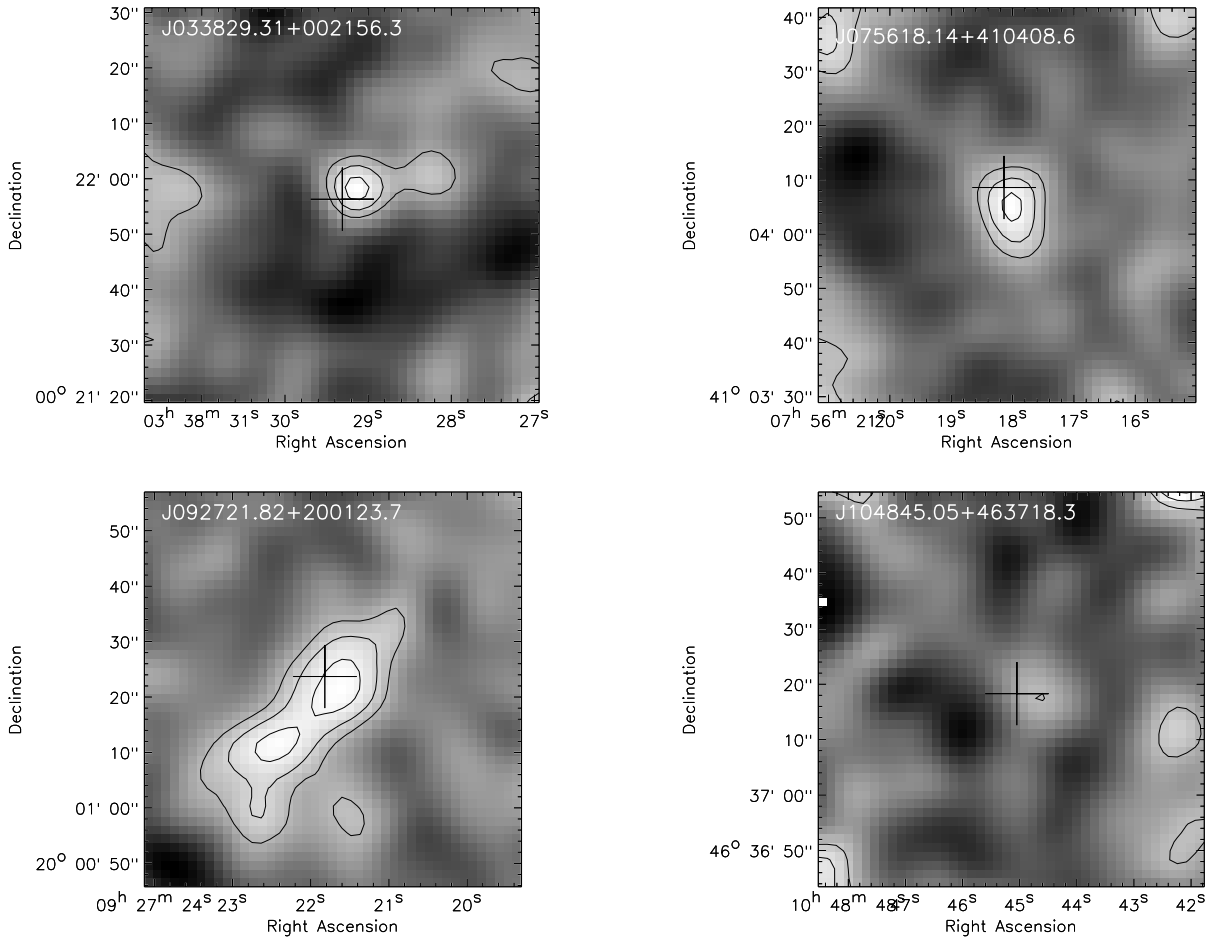

Fig. 1.— The SHARC-II maps of the four z≥5 quasars at 350 μm, smoothing to a beam size of FWHM = 12.4″. The contour levels are $(2, 3, 4) \times 4.0\,\mathrm{mJy\,beam^{-1}}$ for each of the four maps. The crosses mark the positions of the optical quasars.

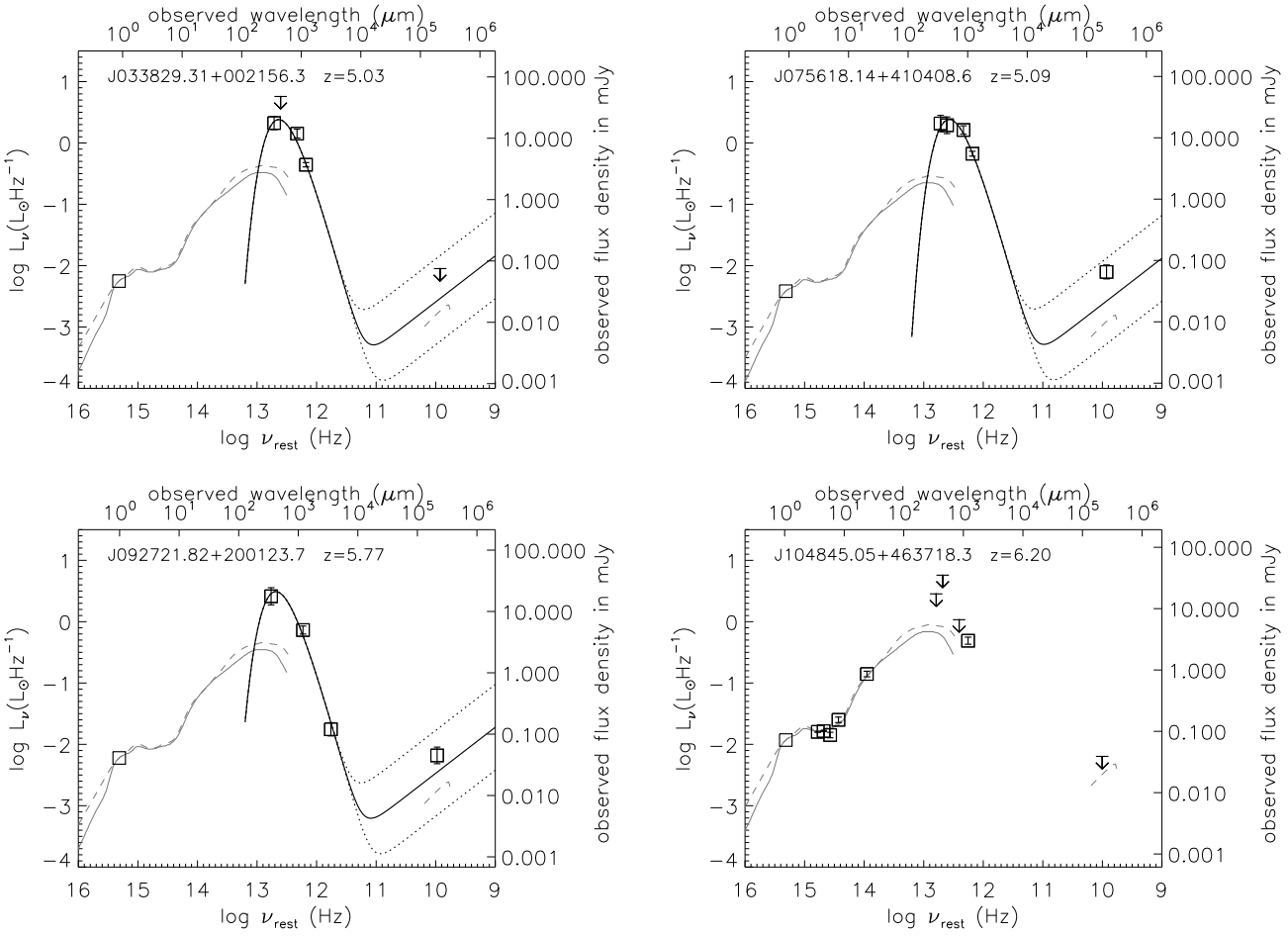

Fig. 2.— Optical to radio SEDs for the four z≥5 quasars. The squares represent optical data at 1450Å, SHARCII data at 350 μm, SCUBA data at 450 μm and 850 μm, MAMBO data at 1.2 mm, PdBI data at 3.5 mm, and VLA data at 1.4GHz. Arrows denote 3σ upper limits for non-detections. The dashed and solid lines represent the low-z quasar templates from Elvis et al. (1994) and Richards et al. (2006), respectively. All the templates are normalized to 1450Å. The hard solid line is the best-fit warm dust model for the three SHARC-II detections, extended to the radio band with the typical radio-FIR correlation of star forming galaxies, i.e. q=2.34 (Yun et al. 2001). The dotted lines denote factors of 5 excesses above and below this typical q value defined by star forming galaxies.

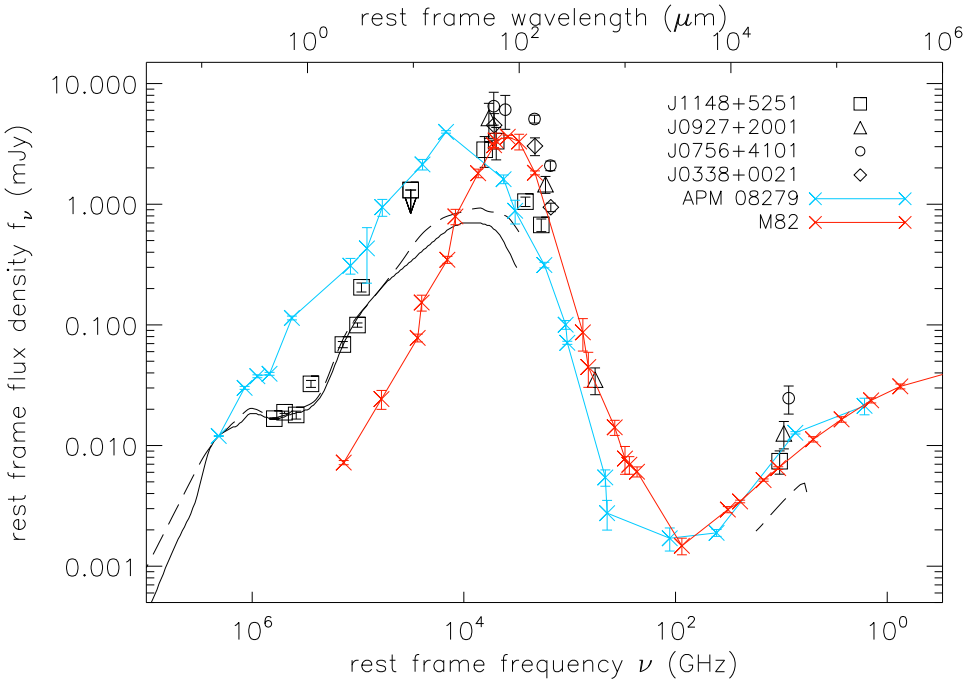

Fig. 3.— Combined rest frame optical to radio SED of the four SHARC-II detected z≥5 quasars. The data of J1148+5251 are taken from Jiang et al. (2006), Charmandaris et al. (2004), Beelen et al. (2006), Robson et al. (2004), Bertoldi et al. (2003a), and Carilli et al. (2004). The flux densities are normalized to the 1450Å emission of J1148+5251. The black lines are quasar templates as described in Figure 2. The blue line is the SED of the z = 3.9 quasar APM 08279+5255, scaling to the 1450Å emission of J1148+5251, with data from Irwin et al. (1998), Lewis et al. (1998, 2002), Downes et al. (1999), Egami et al. (2000), Beelen et al. (2006), Wagg et al. (2005) and Weiβ et al. (2007). The red line is the SED of the central region of the starburst galaxy M82, scaling to the 0.5 mm flux density of the combined SED, with data from Telesco & Harper (1980), Klein et al. (1988), Hughes et al. (1990), Smith et al. (1990), and Krügel et al. (1990).